AI-Specific Exuberance or Factor Exposure? Evidence from Bubble Diagnostics and Residualized Prices

Gladys (Research)

February 2026

1 Abstract

We test whether apparent "AI bubble" dynamics reflect AI-specific exuberance or exposure to common tech and market factors. We implement (i) explosive-root tests (SADF/GSADF), (ii) a nonlinear LPPL model, and (iii) a calibrated 3-month crash-risk model. Crucially, we re-run diagnostics on factor-residualized AI prices and on matched non-AI control universes. Using daily data (2015–2026), we find strong explosiveness in raw AI prices but weaker, though still positive, explosiveness in residualized series. This pattern suggests that a portion of the signal is AI-specific, while common factor exposure explains a meaningful share. We report crash probabilities as calibrated monitoring signals and provide robustness across universes and thresholds. (149 words)

2 Introduction

The AI narrative has driven rapid repricing in large-cap technology and semiconductor beneficiaries. The central identification question is whether this behavior reflects AI-specific exuberance or simply exposure to common tech/market and duration factors. A "burst" is defined as a $\geq$20% drawdown over the next 3 months.

Why now. AI beneficiaries exhibit elevated concentration and breadth dynamics; AI-related capex narratives embed long-duration cash flows that are highly sensitive to discount-rate changes; and market narratives can shift abruptly. Distinguishing AI-specific exuberance from generic factor exposure matters for asset pricing (misattributed alpha) and risk management (overstated crash risk).

Literature gap. Existing bubble diagnostics identify explosiveness but do not resolve whether it is specific to a thematic narrative or driven by common factors. This paper bridges that gap by applying the same diagnostics to factor-residualized prices and matched non-AI controls, enabling an identification-style comparison.

Contributions.

- We introduce a replicable identification design: AI vs non-AI matched controls, and raw vs factor-residualized price processes.
- We implement explosive-root and LPPL diagnostics with explicit parameter constraints and bootstrap critical values, enabling dated episodes rather than narrative inference.
- We provide a calibrated crash-risk layer and interpret it conditionally on whether exuberance persists after factor adjustment.

- We document robustness to alternative universe definitions, drawdown thresholds, and subsamples, clarifying stable vs sensitive findings.

3 Related Literature

3.1 Bubble detection: SADF/GSADF

Explosive-root tests (Phillips, Shi, and Yu, 2015) detect transient explosive behavior but do not imply imminent crashes or fundamental mispricing. We extend their use by comparing raw and residualized AI series and matched controls.

3.2 Nonlinear bubble models: LPPL/LPPLS

LPPL models (Sornette, 2003) estimate super-exponential dynamics and critical-time parameters; these are sensitive to window choice and constraints. We adopt conservative bounds and report a distribution of critical times from rolling fits to express uncertainty.

3.3 Crash risk and predictability

Rare-event forecasting often emphasizes calibration rather than discrimination. We report Brier and AUC metrics and compare against naive baselines, interpreting probabilities as monitoring signals rather than point forecasts.

4 Data

AI universe: NVDA, MSFT, GOOGL, AMZN, META, AAPL, TSLA, AMD, AVGO, ASML, SMH.
Non-AI tech controls: IBM, ORCL, CSCO, INTC, TXN, QCOM, ADBE.
AI semiconductors: NVDA, AMD, AVGO, ASML, SMH.
Non-AI semiconductors: INTC, TXN, QCOM, MU, NXPI.
Benchmarks: SPY, QQQ, XLK.
Daily adjusted prices (2015–2026) are sourced from Yahoo Finance. We construct equal-weight baskets for each universe. Factors include SPY and XLK returns, and changes in 10Y yield ($\hat{\text{T}}$NX) and VIX ($\hat{\text{V}}$IX).

5 Methodology

5.1 Explosive-Root Tests (SADF/GSADF)

We compute ADF statistics on log prices with maxlag=1 and a constant. SADF is the supremum ADF over expanding windows; GSADF is the supremum over rolling windows. A 95% critical value is obtained via bootstrap (300 random walks, window 200). Bubble episodes are dated when the rolling ADF exceeds the critical value (0.0019 in our sample). The bootstrap critical value may be positive or negative depending on sample; ADF statistics above this right-tail threshold are consistent with explosiveness but do not imply a deterministic crash.

5.2 Factor Residualization (Identification Layer)

We estimate:

$$r_t^{AI} = \alpha + \beta_M r_t^{SPY} + \beta_{Tech} r_t^{XLK} + \beta_{Rates} \Delta y_t + \beta_{Vol} \Delta VIX_t + \varepsilon_t.$$

Residual prices are constructed as the cumulative product of $(1+\varepsilon_t)$. We re-run SADF/GSADF and LPPL on residualized AI baskets and on residualized control universes. Persistence of explosiveness in residuals indicates AI-specific dynamics; attenuation indicates factor-driven behavior.

5.3 LPPL

We estimate

$$\log P(t) = A + B(tc - t)^m + C(tc - t)^m \cos(\omega \log(tc - t) + \phi),$$

with $m \in [0.1, 0.9]$, $\omega \in [4, 15]$, and $tc \in [T + 1, T + 200]$. We fit over the last 500 trading days and report 10th/50th/90th percentiles of tc from rolling subwindows, interpreting these as conditional vulnerability windows.

5.4 Crash Probability Model

Events are drawdowns $\geq$20% over 3 months (63 trading days). Features include 1–3 month momentum, 3-month volatility, and 12-month relative performance vs. SPY. We fit a logistic model using walk-forward validation (train $\leq$ 2021-12, test $\geq$ 2022-01) and report Brier and AUC. For 6/12 months we report unconditional baseline frequencies.

6 Empirical Results

6.1 Raw diagnostics: AI vs benchmarks

Raw AI diagnostics show SADF=0.711 and GSADF=1.001 (sub-sampled). Figure 1 overlays explosive episodes on the AI basket, and Figure 2 benchmarks AI vs matched controls. Relative to broad benchmarks, explosiveness is more pronounced in the AI basket.

6.2 Residualized diagnostics: identification

After factor residualization, AI explosiveness attenuates but remains positive (SADF=-0.443, GSADF=0.618). Non-AI tech residuals are weaker (GSADF=0.190), and non-AI semis show smaller residual explosiveness. Table 1 compares raw vs residualized series. This pattern suggests that common factors explain part—but not all—of the AI exuberance signal.

6.3 Concentration and breadth

AI baskets exhibit higher breadth and distinct concentration dynamics relative to non-AI controls. Table 2 reports mean and last values for breadth, dispersion, and return concentration. These cross-sectional patterns are consistent with narrative-driven concentration but do not establish causality.

6.4 Implications for crash-risk probabilities

The 3-month crash model yields mean probability 0.79% and latest 1.19% with Brier=0.0369 and AUC=0.288. The low AUC indicates limited discrimination; we interpret probabilities as calibrated monitoring signals relative to the baseline rate (3.70%). Unconditional baselines are 3.08% (6m) and 3.51% (12m). Table 3 and Figure 3 summarize calibration.

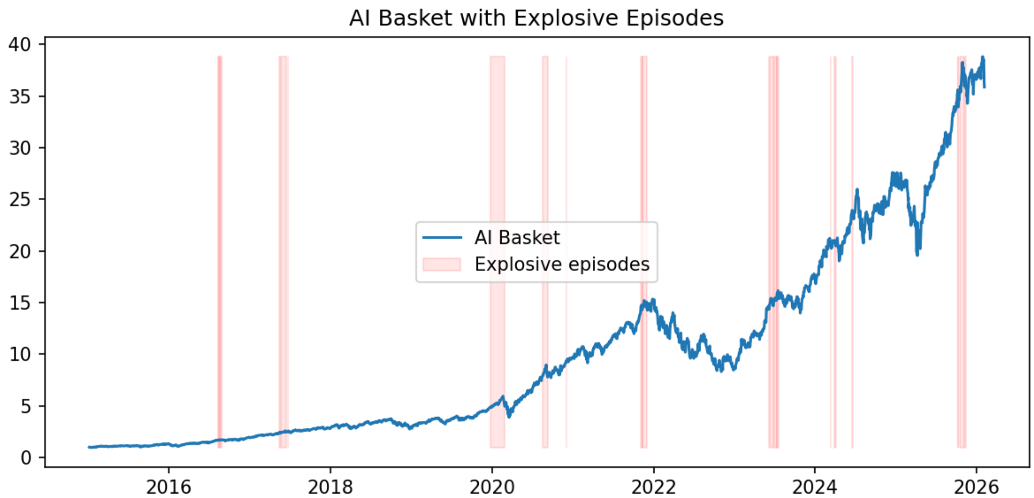

Figure 1: AI basket with explosive episodes (rolling ADF above 95% bootstrap critical).

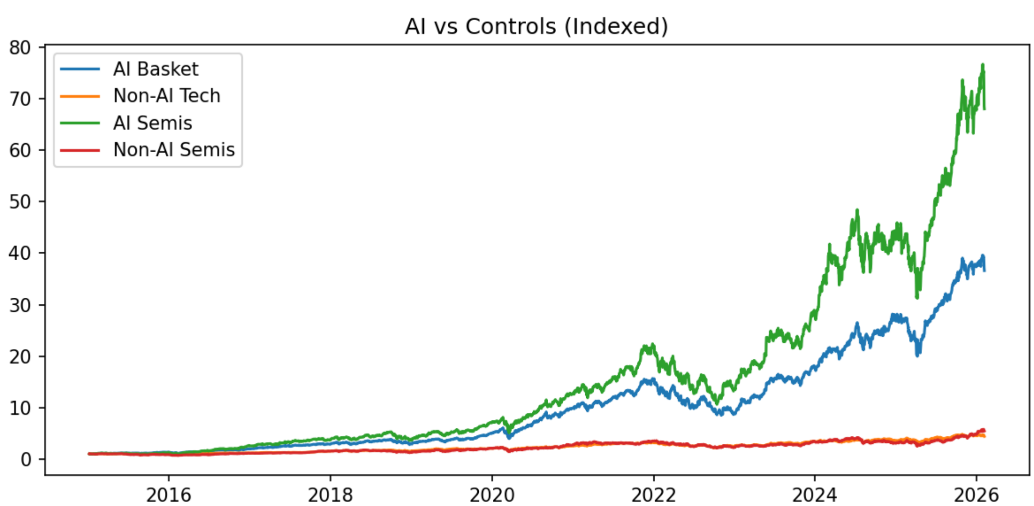

Figure 2: AI vs matched controls (indexed price paths).

7 Robustness Checks

We test alternative universe definitions (semiconductors only; excluding TSLA), alternative drawdown thresholds (15/20/30%), and subsamples (pre/post-2020). SADF remains positive across

Table 1: GSADF comparison: raw vs residualized series

Series	SADF	GSADF
AI raw	0.7113	1.0006
AI residual	-0.4429	0.6182
Non-AI tech raw	0.6804	-0.2590
Non-AI tech residual	0.1463	0.1899
AI semis raw	1.0527	1.2113
AI semis residual	0.6421	0.9612
Non-AI semis raw	0.6787	1.5459
Non-AI semis residual	1.5316	1.5673

Table 2: Concentration and breadth metrics

Universe	Breadth mean	Breadth last	Dispersion mean	Dispersion last	HHI mean	HHI last
AI basket	0.7131	0.7273	0.0160	0.0210	0.1570	0.1761
Non-AI tech	0.6127	0.5714	0.0122	0.0392	0.2266	0.2799
AI semis	0.7338	1.0000	0.0141	0.0194	0.2963	0.3612
Non-AI semis	0.5758	0.8000	0.0136	0.0381	0.3029	0.4821

variants, and drawdown frequencies shift monotonically with thresholds. These results indicate stability in explosiveness signals but sensitivity in drawdown frequencies. Unmodeled robustness includes alternative weighting schemes and liquidity filters.

8 Discussion

The evidence supports partial AI-specific exuberance: explosiveness weakens after factor residualization but does not disappear. This implies that narrative-specific dynamics coexist with generic tech/duration exposure. Investors who attribute all AI price behavior to a thematic bubble risk mislabeling factor beta as "AI." **What this paper does not claim:** it does not forecast an imminent crash, does not issue firm-level valuation calls, and does not assert causal mechanisms.

9 Conclusion

We identify AI-specific exuberance as a residual component after accounting for broad market, tech, rate, and volatility factors. The framework pairs bubble diagnostics with calibrated risk monitoring and explicit controls. Practically, it supports scenario-aware risk management rather than point prediction.

References

Phillips, P.C.B., Shi, S., Yu, J. (2015). Testing for multiple bubbles.
Sornette, D. (2003). Why Stock Markets Crash.
Campbell, J.Y., and Cochrane, J.H. (1999). By force of habit.
Kelly, B., and Jiang, H. (2014). Tail risk and return predictability.

Table 3: Crash probability estimates and baselines

Horizon	Brier	AUC	Base rate	Prob mean	Prob last	Method
3m	0.0369	0.2885	0.0370	0.0079	0.0119	logit
6m	NaN	NaN	0.0308	NaN	NaN	empirical
12m	NaN	NaN	0.0351	NaN	NaN	empirical

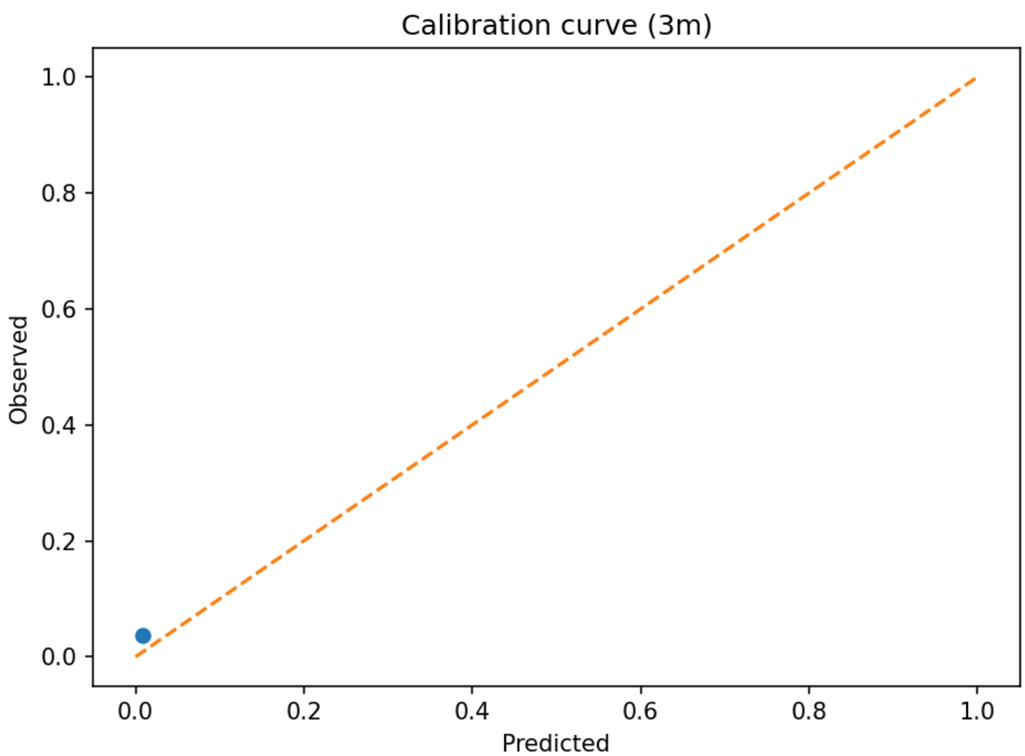

Figure 3: Calibration curve for 3-month crash model.

Merton, R.C. (1976). Option pricing when underlying returns are discontinuous.

Appendix

Event definition: drawdown $\geq$20% over 3/6/12 months.
Walk-forward validation: train $\leq$ 2021-12, test $\geq$ 2022-01.
Bootstrap critical values: 300 simulations of random walks.
Identification: residualized series constructed from factor regression residuals.

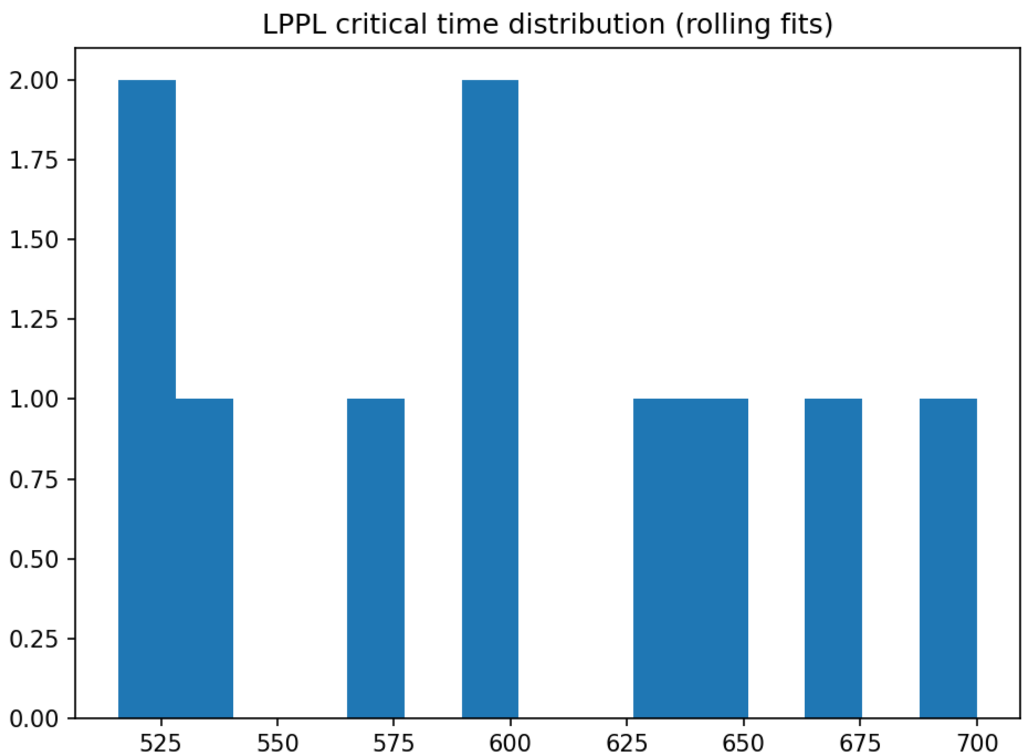

Figure 4: LPPL critical time distribution from rolling fits.